Article

Supramolecular Layer-by-Layer Assembly: Alternating Adsorptions of Guest- and Host-Functionalized Molecules and Particles Using Multivalent Supramolecular Interactions

Olga Crespo-Biel, Barbara Dordi, David N. Reinhoudt, and Jurriaan Huskens

J. Am. Chem. Soc., **2005**, 127 (20), 7594-7600• DOI: 10.1021/ja051093t • Publication Date (Web): 29 April 2005

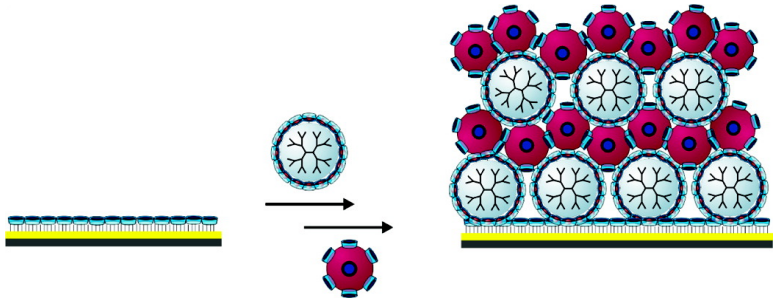

J|A|C|S
ARTICLES
Published on Web 04/29/2005

Supramolecular Layer-by-Layer Assembly: Alternating Adsorptions of Guest- and Host-Functionalized Molecules and Particles Using Multivalent Supramolecular Interactions

Olga Crespo-Biel,[†] Barbara Dordi,[†] David N. Reinhoudt,[†] and Jurriaan Huskens*[,†,‡]

Contribution from the Laboratory for Supramolecular Chemistry and Technology and Strategic Research Orientation "Nanofabrication", MESA+ Institute for Nanotechnology, University of Twente, P.O. Box 217, 7500 AE, Enschede, The Netherlands

Received February 21, 2005; E-mail: j.huskens@utwente.nl

Abstract: The stepwise construction of a novel kind of self-assembled organic/inorganic multilayers based on multivalent supramolecular interactions between guest-functionalized dendrimers and host-modified gold nanoparticles has been developed, yielding supramolecular layer-by-layer assembly. The deposition process was monitored by surface plasmon resonance spectroscopy. Further characterization of the multilayer films was performed by means of UV/vis absorption spectroscopy, which showed a linear increase in absorption with the number of bilayers. The growth of the gold nanoparticle plasmon absorption band corresponded to approximately a dense monolayer of gold nanoparticles per bilayer. Ellipsometry and atomic force microscopy (AFM) scratching experiments were used to measure the development of the film thickness with the number of bilayers, confirming linear growth and a thickness increase of approximately 2 nm/bilayer.

Introduction

The huge interest in nanomaterials has become an important line of research in nanotechnology for the generation of functional molecular assemblies.[1] A prerequisite for the construction of molecule-based functional devices is the development of methods for integrating those molecular components into well-ordered assemblies with a well-defined supramolecular architecture.[2] Such devices require control of molecular orientation and organization at the nanometer scale, and therefore it is essential to study and develop methods for the controlled assembly of multicomponent nanostructures. Numerous examples of supramolecular systems have been previously studied, mainly comprising organized monomolecular films on surfaces.[1c,3] However, the extension of this approach to multilayer films can enhance the properties of monomolecular films and create at the same time a new class of materials possessing functional groups at controlled sites in three-dimensional arrangements.

Initially, the molecularly controlled fabrication of nanostructured films was dominated by the Langmuir−Blodgett (LB) technique, by which monolayers are formed on an air−water interface and then transferred to a solid support.[4,5] However, the LB technique requires special equipment and has limitations with respect to substrate size and topology as well as film quality and stability. Later on, self-assembly techniques[6,7] were developed as an alternative to LB films.

In recent years, layer-by-layer (LBL) assembly[8] has emerged as a promising method for fabricating structured and functional thin films on solid substrates. The LBL method allows one to construct a film atop a substrate of almost any composition or topology by alternating its exposure to solutions containing species of complementary affinities.[9] LBL assembly is mostly achieved by exploiting attractive forces, and by alternating immersions, the multilayer films are attained.[10,11] This method, initially developed to prepare multilayer assemblies electrostatically,[11,12] has been successfully extended to various other driven forces such as hydrogen bonding,[13] charge transfer,[14] acid−base pairs,[15] metal-ion coordination,[16] inter- or intramolecular interactions in the dried state,[17] covalent bonds,[18] biospecific

[†] Laboratory for Supramolecular Chemistry and Technology.
[‡] Strategic Research Orientation "Nanofabrication".

(1) See, for example: (a) Tredgold, R. H. *Order in Organic Films*; Cambridge University Press: Cambridge, U.K., 1994. (b) Parikh, A. N.; Liedberg, B.; Atre, S. V.; Ho, M.; Allara, D. L. *J. Phys. Chem.* **1995**, *99*, 9996−10008. (c) Finklea, H. O. In *Electroanalytical Chemistry*; Bard, A. J., Rubinstein, I., Eds.; Marcel Dekker: New York, 1996; Vol. 19.
(2) Lehn, J.-M. *Supramolecular Chemistry*; VCH Press: New York, 1995.
(3) Ulman, A. *Chem. Rev.* **1996**, *96*, 1533−1554.
(4) Blodgett, K. B. *J. Am. Chem. Soc.* **1934**, *56*, 495−495.
(5) Blodgett, K. B.; Langmuir, I. *Phys. Rev.* **1937**, *51*, 964−982.
(6) (a) Whitesides, G. M. *Chimia* **1990**, *44*, 310−311. (b) Fendler, J. H.; Meldrum, F. C. *Adv. Mater.* **1995**, *7*, 607−632. (c) Colvin, V. L.; Goldstein, A. N.; Alivisatos, A. P. *J. Am. Chem. Soc.* **1992**, *114*, 5221−5230.
(7) For self-assembled monolayers on gold surfaces: (a) Nuzzo, R. G.; Allara, D. L. *J. Am. Chem. Soc.* **1983**, *105*, 4481−4483. (b) Rubinstein, I.; Steinberg, S.; Tor, Y.; Shanzer, A.; Sagiv, J. *Nature* **1988**, *332*, 426−429. For self-assembled monolayers on silicon oxide: (c) Maoz, R.; Sagiv, J. *Langmuir* **1987**, *3*, 1045−1051. (d) Maoz, R.; Sagiv, J. *Langmuir* **1987**, *3*, 1034−1044. (f) Wasserman, S. R.; Tao, Y.; Whitesides, G. M. *Langmuir* **1989**, *5*, 1074−1087.
(8) (a) Decher, G.; Hong, J.-D. *Makromol. Chem., Macromol. Symp.* **1991**, *46*, 321−327. (b) For a review, see: Decher, G. *Science* **1997**, *277*, 1232−1237.
(9) (a) Hammond, P. T. *Curr. Opin. Colloid Interface Sci.* **2000**, *4*, 430−442. (b) Schönhoff, M. *Curr. Opin. Colloid Interface Sci.* **2003**, *8*, 86−95. (c) Decher, G.; Schlenoff, J. B. *Multilayer Thin Films*; Wiley: Weinheim, Germany, 2003.
(10) Decher, G.; Hong, J. D.; Schmitt, J. *Thin Solid Films* **1992**, *210*, 831−835.
(11) For a review on electrostatic LBL assembly: Hammond, P. T. *Adv. Mater.* **2004**, *16*, 1271−1293.

10.1021/ja051093t CCC: $30.25

interactions (e.g., sugar−lectin interactions),[19] and host−guest interactions between cyclodextrin dimers and positively charged ferrocene-appended poly(allylamine) polymers.[20] LBL assembly has been achieved with a large number of materials including polymers,[12] inorganic nanoparticles,[21] clay,[22] organic components,[23] carbon nanotubes,[24] dendrimers,[25] and biological macromolecules such as proteins[26] and DNA.[27]

In our group, we have prepared cyclodextrin (CD) self-assembled monolayers (SAMs) on gold[28] and silicon oxide[29] surfaces onto which stable positioning and patterning of molecules has been achieved by means of multiple supramolecular interactions. Therefore, these CD SAMs constitute a molecular printboard for the positioning of thermodynamically and kinetically stable assemblies of multivalent systems, for example, dendrimers.[30,31] Recently, we showed that an analogous ferrocene-terminated dendrimer (generation 5, 64 ferrocene end groups) binds to CD SAMs on gold with approximately seven interactions to the surface,[32] leaving multiple guest groups exposed to the solution available for complexation of hosts from solution. We have also shown that these molecules bind to the CD printboards with different numbers of interactions depending on the number of functional groups present in the dendrimer.[34,32]

Previously, we have also studied the complexation-induced aggregation in solution of CD-modified gold nanoparticles (CD Au NPs) and adamantyl-functionalized dendrimers.[33] The addition of such a dendrimer to a solution containing CD Au NPs led to pronounced and irreversible precipitation of the dendrimer/CD Au NP aggregates.

Here, we describe the stepwise construction of a novel kind of self-assembled organic/metal NP multilayers on the basis of multivalent supramolecular host−guest interactions between dendritic guest molecules and host-modified gold nanoparticles. Surface plasmon resonance (SPR), ellipsometry, UV/vis, and atomic force microscopy (AFM) have been used for film thickness determination and for monitoring and quantifying the growth process.

Results and Discussion

Multilayer thin films composed of CD-modified gold nanoparticles (CD Au NPs) and adamantyl-terminated dendrimers (generation 5, 64 adamantyl end groups, **1e**; see Chart 1) have been prepared on CD self-assembled monolayers (CD SAMs) using a supramolecular approach. CD SAMs were prepared on gold[28] and on silicon oxide[29] surfaces (Chart 1) following literature procedures. The binding of multivalent guest molecules onto these surfaces has shown that the binding properties of these printboards are practically identical.[29,31,34,35] CD-coated gold nanoparticles (Chart 1) were synthesized according to a literature procedure[36] by reduction of $AuCl_4^-$ in DMSO solution containing perthiolated β-CD.[37] This one-phase procedure is similar to that reported by Brust and co-workers.[38] Using TEM, a mean particle size of 2.8 ± 0.6 nm was found. We chose to use adamantyl-terminated poly(propylene imine) dendrimers because the CD-adamantyl interaction is one of the strongest,[39] the number of adamantyl units (ranging from 4 to 64) can be easily varied, and the spherical shape of the dendrimers allows the multivalent display of these guest functionalities. Dendrimer (Chart 1) **1e** has 64 adamantyl groups and the complexation with CD in solution has been described before.[40]

(12) For some examples: (a) Sukhorukov, G. B.; Möhwald, H.; Decher, G.; Lvov, Y. M. *Thin Solid Films* **1996**, *285*, 220−223. (b) Cheung, J. H.; Stockton, W. B.; Rubner, M. F. *Macomolecules* **1997**, *30*, 2712−2716. (c) Laurent D.; Schlenoff, J. B. *Langmuir* **1997**, *13*, 1552−1557. (d) Caruso, F.; Niikura, K.; Furlong, D. N.; Okahata, Y. *Langmuir* **1997**, *13*, 3422−3426. (e) Hempenius, M. A.; Péter, M.; Robins, N. S.; Kooij, E. S.; Vancso, G. J. *Langmuir* **2002**, *18*, 7629−7634. (f) Cho, J.; Quinn, J. F.; Caruso, F. *J. Am. Chem. Soc.* **2004**, *126*, 2270−2271. (g) Vázquez, E.; Dewitt, D. M.; Hammond, P. T.; Lynn, D. M. *J. Am. Chem. Soc.* **2002**, *124*, 13992−13993. (h) Tian, S.; Baba, A.; Liu, J.; Wang, Z.; Knoll, W.; Park, M.-K.; Advincula, R. *Adv. Funct. Mater.* **2003**, *13*, 473−479.

(13) For some examples: (a) Stockton, W. B.; Rubner, M. F. *Macromolecules* **1997**, *30*, 2717−2725. (b) Yang, S. Y.; Rubner, M. F. *J. Am. Chem. Soc.* **2002**, *124*, 2100−2101. (c) Bai, S.; Wang, Z.; Zhang, X. *Langmuir* **2004**, *20*, 11828−11832. (d) Delongchamp, D. M.; Hammond, P. T. *Langmuir* **2004**, *20*, 5403−5411.

(14) (a) Shimazaki, Y.; Mitsuishi, M.; Ito, S.; Yamamoto, M. *Langmuir* **1997**, *13*, 1385−1387. (b) Wang, X.; Naka, K.; Itoh, H.; Uemura, T.; Chujo, Y. *Macromolecules* **2003**, *36*, 533−535.

(15) Li, D.; Jiang, Y.; Wu, Z.; Chen, X.; Li, Y. *Thin Solid Films* **2000**, *360*, 24−27.

(16) (a) Moav, T.; Hatzor, A.; Cohen, H.; Libman, J.; Rubinstein, I.; Shanzer, A. *Chem. Eur. J.* **1998**, *4*, 502−507. (b) Hatzor, A.; Moav, T.; Cohen, H.; Matlis, S.; Libman, J.; Vaskevich, A.; Shanzer, A.; Rubinstein, I. *J. Am. Chem. Soc.* **1998**, *120*, 13469−13477. (c) Hatzor, A.; Van der Boom-Moav, T.; Yochelis, S.; Vaskevich, A.; Shanzer, A.; Rubinstein, I. *Langmuir* **2000**, *16*, 4420−4423.

(17) Serizawa, T.; Hashiguchi, S.; Akashi, M. *Langmuir* **1998**, *15*, 5363−5368.

(18) Kohli, P.; Blanchard, G. J. *Langmuir* **2000**, *16*, 8518−8524.

(19) (a) Lvov, Y.; Ariga, K.; Ichinose, I.; Kunitake, T. *J. Chem. Soc., Chem. Commun.* **1995**, 2313−2314. (b) Anzai, J.; Kobayashi, Y.; Nakamura, N.; Nishimura, M.; Hoshi, T. *Langmuir* **2000**, *16*, 2851−2856.

(20) Suzuki, I.; Egawa, Y.; Mizukawa, Y.; Hoshi, T.; Anzai, J. *J. Chem. Soc., Chem. Commun.* **2002**, 164−165.

(21) (a) Lvov, Y.; Ariga, K.; Onda, M.; Ichinose, I.; Kunitake, T. *Langmuir* **1997**, *13*, 6195−6203. (b) Cassagneau, T.; Mallouk, T. E.; Fendler, J. H. *J. Am. Chem. Soc.* **1998**, *120*, 7848−7859. (c) Sun, Y.; Hao, E.; Zhang, X.; Yang, B.; Shen, J.; Chi, L.; Fuchs, H. *Langmuir* **1997**, *13*, 5168−5174. (d) Khopade, A. J.; Caruso, F. *Langmuir* **2003**, *19*, 6219−6225. (e) Crisp, M. T.; Kotov, N. A. *Nano Lett.* **2003**, *3*, 173−177. (f) Jiang, C.; Markutsya, S.; Tsukruk, V. V. *Langmuir* **2004**, *20*, 882−890. (g) Tian, S.; Liu, J.; Knoll, W. *Chem. Mater.* **2004**, *16*, 4103−4108. (h) Schneider, G.; Decher, G. *Nano Lett.* **2004**, *4*, 1833−1839.

(22) (a) Glinel, K.; Laschewsky, A.; Jonas, A. M. *Macromolecules* **2001**, *34*, 5267−5274. (b) Zhou, Y. L.; Li, Z.; Hu, N. F.; Zeng, Y. H.; Rusling, J. F. *Langmuir* **2002**, *18*, 8573−8579.

(23) (a) Shen, Y.; Liu, J. Y.; Jiang, J. G.; Liu, B. F.; Dong, S. J. *J. Phys. Chem. B* **2003**, *107*, 9744−9748. (b) Place, I.; Penner, T. L.; McBranch, D. W.; Whitten, D. G. *J. Phys. Chem. A* **2003**, *107*, 3169−3177.

(24) (a) Mamedov, A. A.; Kotov, N. A.; Prato, M.; Guldi, D. M.; Wicksted, J. P.; Hirsch, A. *Nat. Mater.* **2002**, *1*, 190−194. (b) Olek, M.; Ostrander, J.; Jurga, S.; Möhwald, H.; Kotov, M.; Kempa, K.; Giersig, M. *Nano Lett.* **2004**, *4*, 1889−1895. (c) Lahav, M.; Sehayek, T.; Vaskevich, A.; Rubinstein, I. *Angew. Chem., Int. Ed.* **2003**, *42*, 5576−5579.

(25) (a) Tsukruk, V. V.; Rinderspacher, F.; Bliznyuk, V. N. *Langmuir* **1997**, *13*, 2171−2176. (b) Dan, N. *Nano Lett.* **2003**, *3*, 823−827. (c) Khopade, A. J.; Caruso, F. *Nano Lett.* **2002**, *2*, 415−418.

(26) (a) Lvov, Y.; Ariga, K.; Ichinose, I.; Kunitake, T. *J. Am. Chem. Soc.* **1995**, *117*, 6117−6123. (b) Caruso, F.; Möhwald, H. *J. Am. Chem. Soc.* **1999**, *121*, 6039−6046. (c) Panchagnula, V.; Kumar, C. V.; Rusling, J. F. *J. Am. Chem. Soc.* **2002**, *124*, 12515−12521.

(27) (a) Zhou, L. P.; Yang, J.; Estavillo, C.; Stuart, J. D.; Schenkman, J. B.; Rusling, J. F. *J. Am. Chem. Soc.* **2003**, *125*, 1431−1436. (b) Zhou, Y.; Li, Y. *Langmuir* **2004**, *20*, 7208−7214.

(28) De Jong, M. R.; Huskens, J.; Reinhoudt, D. N. *Chem. Eur. J.* **2001**, *7*, 4164−4170.

(29) Onclin, S.; Mulder, A.; Huskens, J.; Ravoo, B. J.; Reinhoudt, D. N. *Langmuir* **2004**, *20*, 5460−5466.

(30) Huskens, J.; Deij, M. A.; Reinhoudt, D. N. *Angew. Chem., Int. Ed.* **2002**, *41*, 4467−4471.

(31) Auletta, T.; Dordi, B.; Mulder, A.; Sartori, A.; Onclin, S.; Bruinink, C. M.; Péter, M.; Nijhuis, C. A.; Beijleveld, H.; Schönherr, H.; Vancso, G. J.; Casnati, A.; Ungaro, R.; Ravoo, B. J.; Huskens, J.; Reinhoudt, D. N. *Angew. Chem., Int. Ed.* **2004**, *43*, 369−373.

(32) Nijhuis, C. A.; Huskens, J.; Reinhoudt, D. N. *J. Am. Chem. Soc.* **2004**, *126*, 12266−12267.

(33) Crespo-Biel, O.; Juković, A.; Karlsson, M.; Reinhoudt, D. N.; Huskens, J. *Isr. J. Chem.* **2005**, in press.

(34) Huskens, J.; Mulder, A.; Auletta, T.; Nijhuis, C. A.; Ludden, M. J. W.; Reinhoudt, D. N. *J. Am. Chem. Soc.* **2004**, *126*, 6784−6797.

(35) Mulder, A.; Auletta, T.; Sartori, A.; Del Ciotto, S.; Casnati, A.; Ungaro, R.; Huskens, J.; Reinhoudt, D. N. *J. Am. Chem. Soc.* **2004**, *126*, 6627−6636.

(36) Liu, J.; Ong, W.; Román, E.; Lynn, M. J.; Kaifer, A. E. *Langmuir* **2000**, *16*, 3000−3002.

(37) Rojas, M. T.; Königer, R.; Stoddart, J. F.; Kaifer, A. E. *J. Am. Chem. Soc.* **1995**, *117*, 336−343.

(38) Brust, M.; Bethell, D.; Schiffrin, D. J.; Kiely, C. *J. Chem. Soc., Chem. Commun.* **1995**, 1655−1656.

(39) For a general review on cyclodextrins, see: *Chem. Rev.* **1998**, *98*, volume 5. For a list with typical guest molecules, see: Rekharsky, M. V.; Inoue, Y. *Chem. Rev.* **1998**, *98*, 1880−1901.

Chart 1. Chemical Structures of the Host Adsorbates, the CD Au NPs, and Adamantyl-Terminated PPI Dendrimers (**1**) Used in This Study

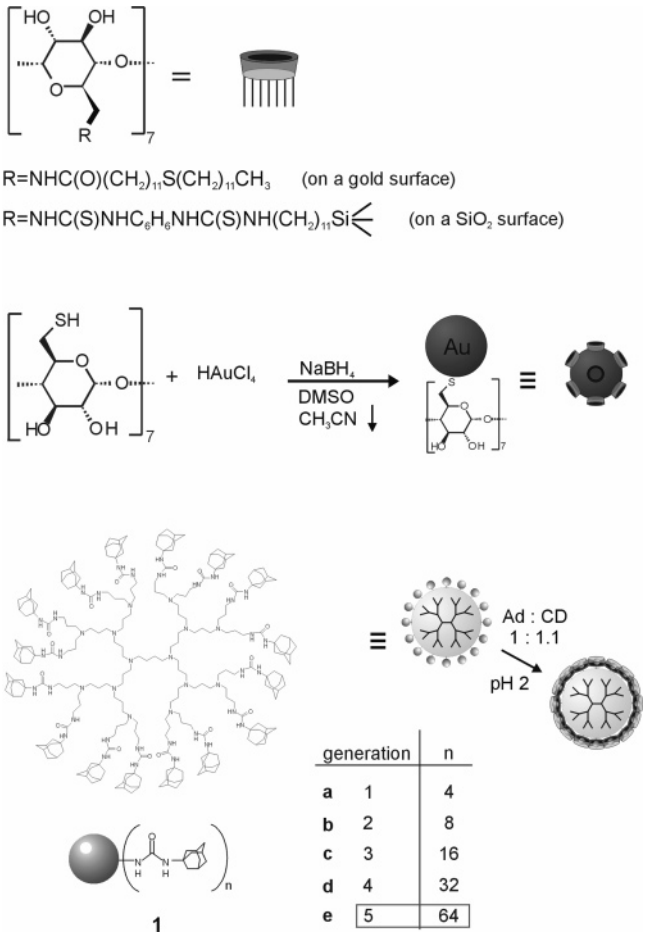

Scheme 1. Layer-by-Layer Assembly Scheme for the Alternating Adsorption of Adamantyl-Terminated PPI Dendrimer **1e** and CD Au NPs onto CD SAMs

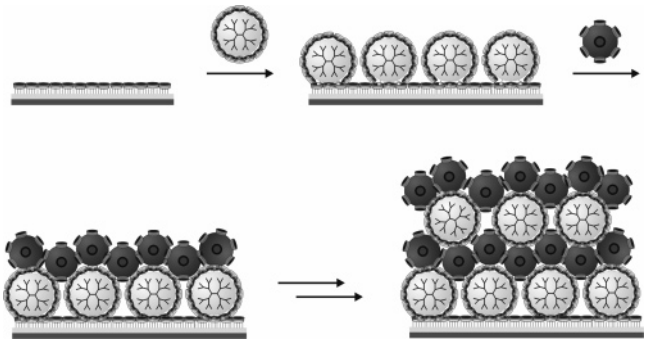

The LBL assembly of dendrimer **1e** and CD Au NPs is shown in Scheme 1. The idealized layer order in this scheme does not reflect a possible intermixing of the layers after adsorption; it merely reflects the sequential adsorption steps. Throughout this paper, the concentration of the two components is expressed as the concentration of functional substituents, that is, of CD and Ad groups. The multilayers were deposited onto CD SAMs on gold[28] and on SiO_2.[29]

Adamantyl-terminated PPI dendrimers were insoluble in water, but by complexation of the adamantyl end groups by slight excess of cyclodextrin and by the protonation of the dendrimer core amine functionalities, they could be brought into aqueous (pH = 2) solution.[40] However, at pH > 7, precipitation of generations 3−5 of these PPI dendrimers occurs. Conversely, CD Au NPs are not stable in acidic solution. Therefore, the LBL assembly was typically accomplished by alternately dipping the substrate into a solution of **1e** in aqueous acidic 1 mM CD (pH = 2) solution, followed by rinsing the substrate with the same 1 mM CD (pH = 2) solution, and into an aqueous CD Au NPs solution, followed by rinsing with water. The delivery of the dendrimers from solution-phase CD complexes to the CD SAMs makes use of the competition between the solution and the surface host sites, as well as the multivalency of the surface host sites emerging from the surface immobilization.[30,31]

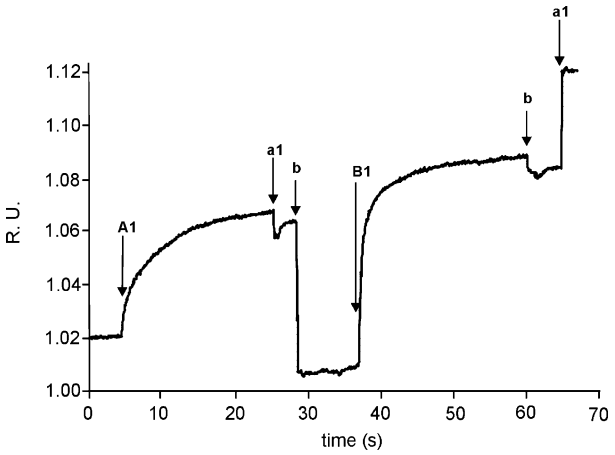

Figure 1. Surface plasmon resonance (SPR) spectroscopy time traces for the adsorption of one bilayer of **1e** (0.01 mM in hydrophobic moieties in a 1 mM CD solution, pH 2) and CD Au NPs (5.8 μM in CD moieties in water) onto a CD SAM on gold; solutions: A1: **1e**; B1: CD Au NPs; a1: 1 mM CD, pH 2; b1: water.

The supramolecular LBL film formation was studied in situ by surface plasmon resonance (SPR) spectroscopy. SPR titrations were performed in the presence of water or 1 mM CD pH 2 as the background, depending on which of the two components was added (see above). The formation of one bilayer is illustrated in Figure 1, where the SPR reflectivity changes upon injection of an aqueous solution of **1e** (A1; vs a background (a1) of 1 mM CD pH 2) and CD Au NPs (B1; vs a background (b) of water), are shown. After the injection of each component, the adsorption was followed for 20−25 min by rinsing of the cell with the corresponding backgrounds 1 mM CD pH 2 (a1) after A1 and water (b) after B1 to remove nonspecifically adsorbed material. In the SPR experiments, the background is switched before the actual injection of the other component (b before B1 and a1 before A1) to allow quantitative comparison of both adsorption steps with subsequent bilayer formation steps.

The SPR-monitored multilayer formation is shown in Figure 2, where six to seven bilayers were successfully accomplished. SPR titrations were performed at different concentrations of the components (shown in Figure 2: left: 0.1 mM in hydrophobic moieties for **1e** and 58 μM in CD moieties for CD Au NPs and right: 0.01 mM **1e** and 5.8 μM CD Au NPs) with the aim to find the right conditions for the supramolecular LBL assembly. The top graphs show the SPR sensograms, while the bottom graphs show the reflectivities as a function of the number of bilayers.

(40) Michels, J. J.; Baars, M. W. P. L.; Meijer, E. W.; Huskens, J.; Reinhoudt, D. N. *J. Chem. Soc., Perkin Trans. 2* **2000**, 1914−1918.

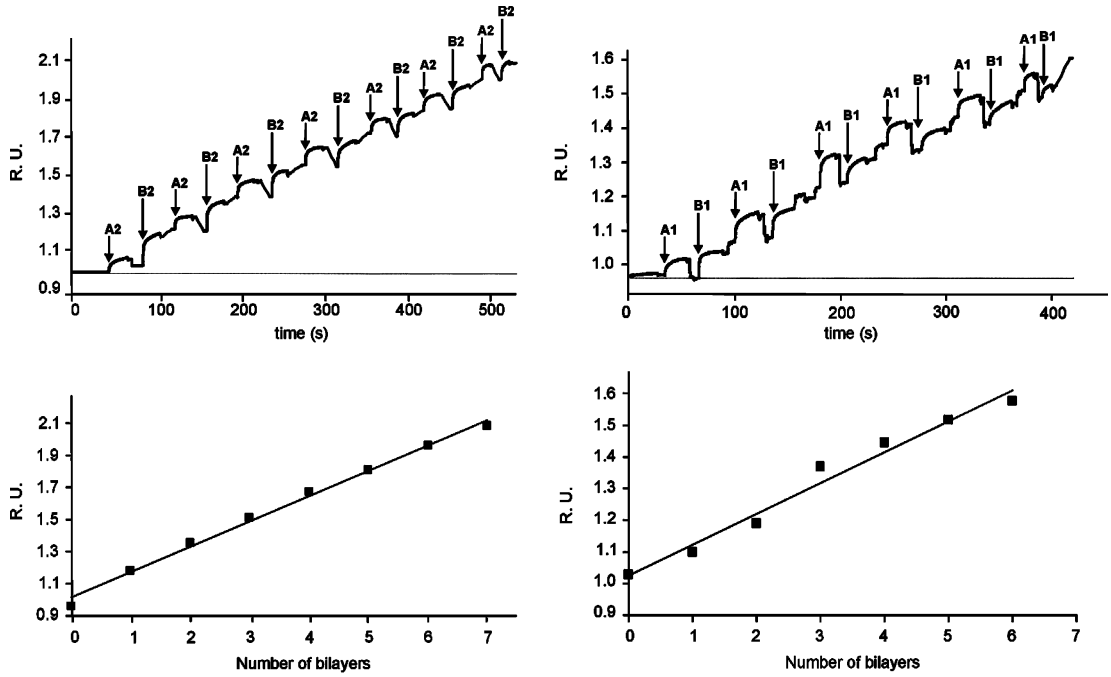

Figure 2. Top: SPR time traces for the LBL assembly process of **1e** (left, A2: 0.1 mM; right, A1: 0.01 mM, in a 1 mM CD pH 2 solution) and CD Au NPs (left, B2: 58 μM; right, B1: 5.8 μM, in water) onto CD SAMs on gold. Bottom: SPR reflectivity changes as a function of the number of bilayers of **1e** and CD Au NPs on CD SAMs on gold.

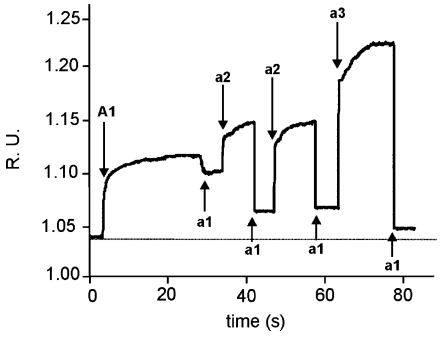

Figure 3. SPR time traces of the adsorption and attempted desorption of **1e** (0.01 mM) onto an oligo(ethylene glycol) SAM; solutions: A1: 0.01 mM **1e**; a1: 1 mM CD pH 2; a2: 5 mM CD pH 2; a3: 10 mM CD pH 2.

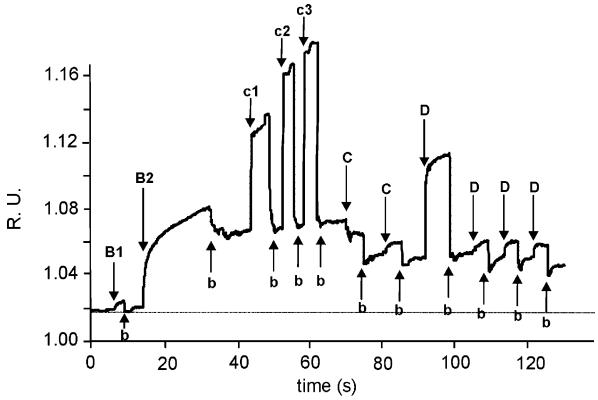

Figure 4. SPR time traces of the adsorption and attempted desorption of CD Au NPs onto a CD SAM; solutions: B1: 5.8 μM CD Au NPs; B2: 58 μM CD Au NPs; b: H_2O; c1: 50 mM NaCl; c2: 100 mM NaCl; c3: 1 M NaCl; C: 1 mM sodium 1-adamantylcarboxylate; D: 5 mM 1-adamantylamine.

As shown in Figure 2, the adsorption behavior was observed to be similar at these concentrations. The bottom graphs show that the growth is linear with the number of bilayers deposited onto the CD SAMs for both concentrations. The slopes of the lines indicate that 10 times higher concentrations of both dendrimers and CD Au NPs lead to only about 1.5 times more adsorption, clearly confirming the supramolecular specificity of binding. For even higher concentrations, physisorption of, in particular, the CD Au NPs appeared to be more severe, while for lower concentrations adsorption of the dendrimer appeared to become too slow because of severe diffusion limitation.

Titrations performed with **1e** (0.01 mM) on an oligo(ethylene glycol)[41] SAM (lacking the host sites) showed nonspecific adsorption of **1e**, which could be reversed by copious rinsing with concentrated CD solutions (Figure 3). As illustrated in Figure 4, the adsorption of a low concentration of CD Au NPs (5.8 μM) (B1) onto a CD SAM showed a small refractive index effect on the SPR signal, which could be instantaneously restored by rinsing with water. However, injection of a higher concentration of CD Au NPs (58 μM) (B2) showed nonspecific adsorption, and extensive rinsing of the cell with water and salt solutions did not completely restore the signal. Even after rinsing with monovalent guests, sodium 1-adamantylcarboxylate (C), and 1-adamantylamine (D), more than 50% of the CD Au NPs remained on the surface. However, as has been observed in Figure 2, the LBL assembly for both CD Au NPs concentrations gave comparable SPR reflectivity changes, thus indicating that both concentrations are suitable for the LBL assembly. Apparently, the nonspecific adsorption of the CD Au NPs on a layer of already adsorbed Au CD NPs is significantly less severe than on a bare CD SAM.

Information on the absolute film thickness increase with the number of bilayers was obtained from ellipsometry, using CD SAMs on SiO_2. Figure 5 shows the ellipsometric thickness as a function of the number of deposited bilayers. The starting 3

(41) Pale-Grosdemange, C.; Simon, E. S.; Prime, K. L.; Whitesides, G. M. *J. Am. Chem. Soc.* **1991**, *113*, 12−20.

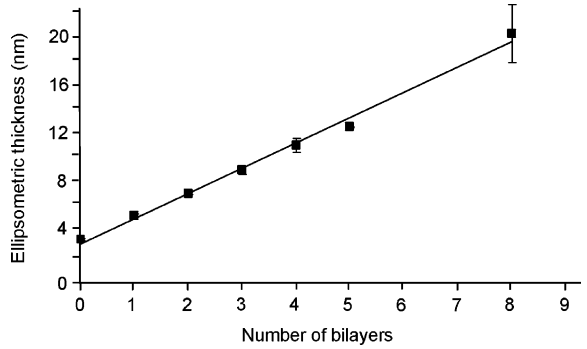

Figure 5. Ellipsometric thicknesses as a function of the number of bilayers of **1e** (0.1 mM in a 1 mM CD solution, pH 2) and CD Au NPs (58 μM in water) onto a CD SAM on silicon oxide.

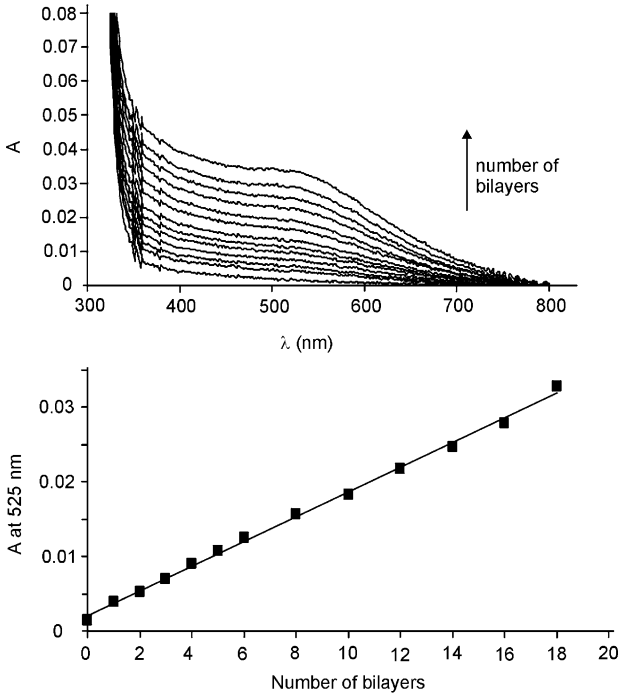

Figure 6. UV/vis absorption spectra (top) and absorbance at 525 nm (bottom) as a function of the number of bilayers of **1e** (0.1 mM in a 1 mM CD solution, pH 2) and CD Au NPs (58 μM in water) onto a CD SAM on glass.

nm for the CD SAM confirms our earlier data.[29] The thickness of the multilayer film (estimating using a refractive index of 1.500 for the organic/metal layers and 1.457 for the underlying native oxide) follows a linear behavior with the number of bilayers, in accordance with the SPR results. The line fit indicates a thickness increase of about 2 nm/bilayer. The exact value of the real part of the multilayer refractive index is not known, and hence higher accuracies cannot be obtained.

UV/vis spectroscopy was used to monitor the supramolecular assembly of the CD Au NPs on a glass surface. Dendrimer adsorption was not visible in the visible region. When CD Au NPs were adsorbed onto the film, the CD Au NPs plasmon absorption band in the visible region emerged at around 525 nm similar to the CD Au NPs in solution.[33] Figure 6 (top) shows the UV/vis absorption spectra of the multilayer **1e**/CD Au NPs films for different numbers of bilayers on a CD SAM. The increase in absorption at 525 nm as a function of the number of bilayers deposited on the CD surface is shown in Figure 6 (bottom). An essentially linear dependence was found, confirming the SPR and ellipsometry data. The linearity was shown to last up to 18 bilayers, which is a strong indication of a well-defined deposition process.[8b,9c]

UV/vis spectroscopy can give a quantitative estimate of the amount of material deposited after each cycle, when it is assumed that the plasmon band extinction coefficients are identical in solution and in the multilayer architecture. On the basis of previous results[33] on aggregation of these CD Au NPs with dendrimers in solution, this assumption seems justified. From the absorption at 525 nm of a solution of 0.29 mg/cm^3 (58 μM in CD moieties) CD Au NPs, the extinction coefficient, ϵ, was calculated to be 0.586 cm^2/mg using the Lambert−Beer law. From the slope (0.001607) of Figure 6 (bottom), the surface coverage for one layer of CD Au NPs was calculated to be 3.1 μg/cm^2. A theoretical value of 1.7 μg/cm^2 was estimated on the basis of the formation of a monolayer of CD Au NPs in a hexagonal packing with a lattice periodicity of a gold NP core summed with twice the CD cavity height[42] and taking into account that the gold core contributes 62% of the total weight of the Au NPs.[33] Thus, the experimental value is a factor 1.8 larger than the crude theoretical estimate obtained assuming a hexagonal packing of monodisperse particles. Most of this difference can probably be attributed to the slight physisorption of the CD Au NPs at the relatively high concentration employed in the UV/vis experiments (compare to SPR results shown in Figure 2 and discussed above). Nevertheless, the fair comparison between the experimental and the theoretical values clearly indicates that close to a monolayer of Au NPs is deposited after each deposition cycle.

AFM was used for a direct determination of the thickness of the multilayer thin film.[43] The LBL assembly was achieved by the alternating immersion of a CD SAM on an annealed gold substrate into the dendrimer and CD Au NPs solutions (0.01 mM for **1e** and 5.8 μM for CD Au NPs) with rinsing steps in-between. The AFM tip was used to create a scratch down to the gold, and the thickness was determined by scanning across the scratch with the AFM tip. The thickness was determined on different samples with one to six bilayers. The multilayer thickness as a function of the number of deposited bilayers is shown in Figure 7, demonstrating that the thickness of the film is linearly related to the number of deposited bilayers, thus corroborating the previous results. An estimate of the multilayer thickness of 2 nm/bilayer was obtained in congruence with the ellipsometry results.

Conclusions

A supramolecular procedure was introduced for the stepwise construction of multilayer thin films. The procedure, based on the LBL assembly of guest-functionalized dendrimers and CD Au NPs, was demonstrated to yield multilayer thin films with thickness control at the nm level. Characterization by means of SPR, UV/vis spectroscopy, ellipsometry, and AFM showed a

(42) The lattice constant was calculated assuming monodisperse CD Au NPs of 2.8 nm in core diameter, adding twice the cyclodextrin cavity height of 0.8 nm. The total weight of the CD Au NPs is constituted of gold (62%), cyclodextrin(25%), and water (13%) (see ref 33). The hexagonal packing on the surface gives the maximal surface coverage possible for a well-packed self-assembled monolayer of a monodisperse sample of nanoparticles, assuming the formation of specific interactions only.

(43) Lobo, R. F. M.; Pereira-da-Silva, M. A.; Raposo, M.; Faria, R. M.; Oliveira, O. N., Jr. *Nanotechnology* **1999**, *10*, 389−393.

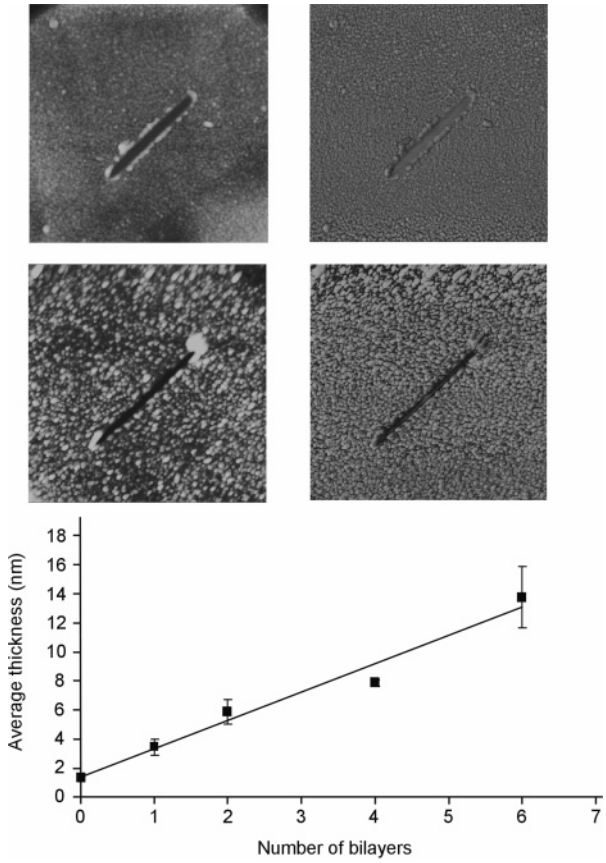

Figure 7. TM-AFM height (top left, *z* range 20.0 nm; center left, *z* range 10.0 nm) and phase (top right, *z* range 50.0°; center right, *z* range 80.0°) images ($\times 1.2\ \mu m^2$) in air of one bilayer (top) and four bilayers (center) on a CD SAM after LBL assembly (**1e**, 0.01 mM in hydrophobic moieties in a 1 mM CD pH 2 solution, and CD Au NPs, 5.8 μM in water). Bottom: Multilayer thickness as a function of the number of bilayers measured with AFM scratching experiments.

well-defined multilayer formation, an accurate thickness control, and the need of specific host−guest interactions.

Such protocols can potentially be used for obtaining various structures, whose assembly is driven by multiple supramolecular interactions. This constitutes a general nanofabrication paradigm for the integration of organic, inorganic, metallic, and biomolecular components while retaining the interfacing supramolecular specificity. The ultimate *z* control, when combined with top-down surface patterning strategies such as soft lithography[11] for *x*,*y* control, can lead to 3D nanofabrication schemes.

Experimental Section

Materials. Chemicals were obtained from commercial sources and used as such. β-Cyclodextrin (CD) was dried in a vacuum at 80 °C in the presence of P_2O_5 for at least 5 h before use. Solvents were purified according to standard laboratory methods.[44] Perthiolated β-CD[37] and per-6-amino-β-cyclodextrin[45] were synthesized according to literature procedures. Milli-Q water with a resistance larger than 18 MΩ was used in all our experiments. Generation 5 adamantyl-terminated poly(propylene imine) (PPI) dendrimer (with 64 adamantyl groups) was synthesized as reported before.[46] Synthesis of the β-cyclodextrin heptathioether adsorbate was reported previously.[28] 1-Mercaptoundec-11-yl-tetra(ethylene glycol) was synthesized according to a literature procedure.[41] CD-coated gold nanoparticles were synthesized according to literature procedure,[36] by the reduction of $HAuCl_4$ in DMSO by $NaBH_4$ in the presence of per-6-thio-cyclodextrin.[37] The CD Au NPs were characterized by UV/ vis spectroscopy, ^{1}H NMR, transmission electron microscopy (TEM), and thermogravimetric analysis (TGA). Using TEM, a mean particle size of 2.8 ± 0.6 nm was found.[33] NMR spectra were recorded on Varian AC300 and AMX400 spectrometers. FAB-MS spectra were recorded with a Finnigan MAT 90 spectrometer using m-NBA as the matrix.

Substrate and Monolayer Preparation. All glassware used to prepare monolayers was immersed in piraña (concentrated H_2SO_4 and 33% H_2O_2 in a 3:1 ratio). (Warning! Piraña should be handled with caution; it has detonated unexpectedly.) The glassware was rinsed with large amounts of high purity water (Millipore). All solvents used in monolayer preparation were of p.a. grade. All adsorbate solutions were prepared freshly prior to use. Round glass-supported gold substrates for SPR (2.54-cm diameter; 47.5 nm Au) and gold substrates for AFM (20 nm of gold on a glass substrate) were obtained from Ssens BV (Hengelo, The Netherlands). Gold substrates were cleaned by immersing the substrates in piraña for 5 s and leaving the substrates for 5 min in absolute EtOH.[47] Gold substrates used in the AFM scratching experiments were flame-annealed in a H_2 flame. The substrates were subsequently immersed into a 0.1 mM β-CD heptathioether adsorbate solution in EtOH and $CHCl_3$ (1:2 v/v) for 16 h at 60 °C. SAMs of 1-mercaptoundec-11-yl-tetra(ethylene glycol) were adsorbed from EtOH at room temperature for 24 h. The samples were removed from the solution and rinsed with substantial amounts of chloroform, ethanol, and Milli-Q water. Silicon oxide substrates were exposed to a cooled (3−7 °C) 0.1 vol % solution of 1-cyano-11-trichlorosilylundecane (purchased from Gelest Inc.) in freshly distilled toluene for 35 min under N_2. Following monolayer formation,[29] the substrates were rinsed with toluene to remove any excess of silanes and were subsequently dried in a stream of nitrogen. The cyano-terminated SAMs were reduced to amines, and transformation of the amine-terminated SAMs to isothiocyanate-bearing layers was accomplished by exposure to a solution of 1,4-phenylene diisothiocyanate. CD-terminated SAMs were finally obtained by reaction of the isothiocyanate-terminated monolayer with per-6-amino-β-cyclodextrin.[45]

Multilayer Formation. The CD SAM substrates were immersed into the solution of **1e** dendrimer for 10 min, followed by rinsing with 1 mM CD at pH = 2. The films were then immersed in the CD Au NPs solution for 10 min, followed by rinsing with water. A multilayer structure was formed by repeating both adsorption steps in an alternating manner. For SPR measurements, titrations were performed starting with a buffer solution (a1, 1 mM CD pH 2) in the cell which was replaced by a solution of dendrimer **1e**. After addition of **1e**, the cell was thoroughly rinsed with 1 mM CD pH 2 followed by rinsing with water. After stabilization of the SPR signal, cell solution was replaced by a CD Au NPs solution followed by extensive rinsing with water and then switching back to the original CD solution (a1). The same procedure was repeated until the required number of bilayers was achieved.

Surface Plasmon Resonance. The SPR setup was obtained from Resonant Probes GmbH.[48] A light beam from the HeNe laser (JDS Uniphase, 10 mW, λ = 632.8 nm) passes through a chopper that is connected to a lock-in amplifier (EG&G, 7256). The modulated beam then passes through two polarizers (Owis), by which the intensity and the plane of polarization of the laser can be adjusted. The modulated beam passes a beam-expanding unit (spatial filter) with a pinhole (25 μm) for spectral cleaning of the wave fronts. The light is coupled via a high index prism (Scott, LaSFN9) in this Kretschmann configuration

(44) Perrin, D. D.; Armarego, W. F. L. *Purification of Laboratory Chemicals*, 3rd ed.; Pergamon: Oxford, U.K., 1989.
(45) Ashton, P. R.; Königer, R.; Stoddart, J. F.; Alker, D.; Harding, V. D. *J. Org. Chem.* **1996**, *61*, 903−908.
(46) Baars, M. W. P. L.; Karlsson, A.; Sorokin, V.; De Waal, B. F. M.; Meijer, E. W. *Angew. Chem., Int. Ed.* **2000**, *39*, 4262−4265.
(47) Ron, H.; Rubinstein, I. *Langmuir* **1994**, *10*, 4566−4573.
(48) Aust, E. F.; Ito, S.; Sawondny, M.; Knoll, W. *Trends Polym. Sci.* **1994**, *2*, 313−323.

to the (Au) metal-coated substrate which is index-matched to the prism in contact with a Teflon cell having O-rings for a liquid-tight seal. The sample cell is mounted on top of a θ-2θ goniometer with the detector measuring the reflectivity changes as a function of the angle of incidence of the p-polarized incoming laser beam. The incoming s/p laser beam passes through a beam splitter, which splits the p- and the s-polarized light. The s-polarized light is conducted to a reference detector. The p-polarized light passes a beam-expanding unit (spatial filter) with a pinhole (25 μm) for spectral cleaning and control of the intensity of p-polarized light and is collected into a photodiode detector. The multilayer formation was measured in real time by recording the changes in the reflectivity in the fixed angle mode (55.2°).

UV/vis Spectroscopy. Multilayers were deposited on a CD-modified glass substrate. UV/vis spectra were recorded on a Varian Cary 300 Bio instrument in double-beam mode, using an uncovered glass slide as a reference. The glass slide was placed perpendicular to the beam to maintain the same positioning during each measurement.

Ellipsometry. Ellipsometric measurements were performed on a Plasmon ellipsometer ($\lambda = 633$ nm) assuming a refractive index of 1.500 for the organic/metal multilayers and 1.457 for the underlying native oxide. The thickness of the SiO_2 layer was measured separately on an unmodified part of the same wafer and subtracted from the total layer thickness determined for the monolayer-covered silicon substrate. Optical measurements were performed after deposition of every bilayer on the same substrate, without changing the parameters of the ellipsometer.

AFM. The AFM measurements were carried out on multilayer structures adsorbed on CD SAMs on flame-annealed gold substrates in tapping mode with a Nanoscope III multimode AFM (Digital Instrument, Santa Barbara, CA) using silicon cantilever/tip (Nanosensor, Wetzlar, Germany; cantilever resonance frequency $f_0 = 280-320$ kHz). A sample area of 500 × 500 nm was scanned by a silicon tip with a radius in the range of 5−10 nm, with a frequency of 1.5 Hz. The furrow was produced with the slow scanning motion disabled by gradually increasing the tip−sample interaction in steps of 0.5 V of the amplitude setpoint, after each four scanning cycles. To easily locate the furrow and produce a better resolution, the scan size was increased and the scan direction was set to 45°. The samples were prepared on annealed gold.

Acknowledgment. We are grateful to the Council for Chemical Sciences of The Netherlands Organization for Scientific Research (NWO-CW) for financial support in the Young Chemists program (O.C.B.; grant 700.50.522 to J.H.). We thank Christian A. Nijhuis for the synthesis of **1e** and 1-mercaptoundec-11-yl-tetra(ethylene glycol).

JA051093T